

EMBEDDED LARGE-SCALE HANDWRITTEN CHINESE CHARACTER RECOGNITION

Youssef Chherawala, Hans J.G.A. Dolfing, Ryan S. Dixon, and Jerome R. Bellegarda

Apple Inc., Cupertino, California 95014, USA

ABSTRACT

As handwriting input becomes more prevalent, the large symbol inventory required to support Chinese handwriting recognition poses unique challenges. This paper describes how the Apple deep learning recognition system can accurately handle up to 30,000 Chinese characters while running in real-time across a range of mobile devices. To achieve acceptable accuracy, we paid particular attention to data collection conditions, representativeness of writing styles, and training regimen. We found that, with proper care, even larger inventories are within reach. Our experiments show that accuracy only degrades slowly as the inventory increases, as long as we use training data of sufficient quality and in sufficient quantity.

Index Terms— Chinese handwriting recognition, style diversity, neural architecture optimization, mobile devices

1. INTRODUCTION

Online handwriting input has recently become more prevalent given the pervasiveness of mobile phones, tablets, and wearable gear like smartwatches. For Chinese in particular, it can significantly enhance user experience given the relative complexity of keyboard methods. Chinese handwriting recognition is uniquely challenging, due to the large number of distinct entries in the underlying character inventory. Unlike alphabet-based writing, which typically involves on the order of 100 symbols, the standard set of Hànzì characters in Chinese National Standard Guójīā Biāozhǔn GB18030–2005 contains 27,533 entries, and many additional logographic characters are in use throughout Greater China.

For computational tractability, it is usual to focus on a restricted number of “commonly used” characters. The standard GB2312-80 set only includes 3,755 (level-1) and 3,008 (level-2) entries, for a total of 6,763 characters. The closely aligned character set used in the popular CASIA databases comprises a total of 7,356 entries [10]. The handwritten database SCUT-COUCH has similar coverage [12]. At the individual user level, however, what is “commonly used” typically varies somewhat from one person to the next. Most people need at least a handful of characters deemed “infrequently written,” as they happen to occur in the compendium of proper names that is relevant to them. Thus ideally we would need to scale up to at least the level of GB18030-2005.

While early recognition algorithms mainly relied on structural methods based on individual stroke analysis, the need to achieve stroke-order independence later sparked interest into statistical methods using holistic shape information [9]. This obviously complicates large-inventory recognition, as correct character classification tends to get harder with the number of categories to disambiguate [5]. On Latin script tasks such as MNIST [8], convolutional neural networks (CNNs) soon

emerged as the approach of choice [15]. Given a sufficient amount of training data, supplemented with synthesized samples as necessary, CNNs decidedly achieved state-of-the-art results [1, 13]. The number of categories in those studies, however, was by nature very small (10).

Applying CNNs to the large-scale recognition of Chinese characters thus requires careful consideration of the underlying character inventory. This is particularly true if the recognition system is to perform inference in real-time on mobile devices. This paper focuses on the challenges involved in terms of accuracy, character coverage, and robustness to writing styles. We investigate and adapt recent advances in CNN architecture design for the unique challenges of large datasets, in order to produce practical models which can be deployed in commercial applications. Section 2 presents the CNN architecture we adopted. Section 3 focuses on the challenges involved in scaling up the system to a larger inventory. Section 4 describes our experiments and presents comparative results obtained on the CASIA database. Finally, Section 5 concludes with some prognostications regarding a possible evolution to the full Unicode inventory.

2. MODEL ARCHITECTURE

We adopt the MobileNetV2 CNN architecture [14] and adapt it to our Chinese handwriting recognition task, due to: (i) impressive accuracies observed for image classification, and (ii) real-time performance on mobile devices. The first aspect can be traced to both residual connections [3], which allow training of deeper and more accurate networks, and batch normalization [7], which enables faster model convergence during training while acting as a regularizer. The second aspect involves replacing standard convolutions with depthwise separable convolutions [6], which reduce by an order of magnitude the number of operations needed. In addition, MobileNetV2 relies on the so-called (inverted) *bottleneck block*, which further reduces memory requirements at inference time. The number of channels of the input of the block is first increased by an expansion factor t before performing the convolution and compressed back at the output of the block. Maintaining the compressed form of the input in memory for the residual connection reduces the memory footprint.

Our adapted version of MobileNetV2 is shown in Fig. 1, with the *block sequence* as main building block. Each such block is itself a sequence of n bottleneck blocks. Only the first bottleneck block of each sequence performs spatial sub-sampling by using a stride of 2. The remaining bottleneck blocks have residual connections between their input and outputs. Different bottleneck blocks can be sequences of different lengths. The input of the network is a medium-resolution image (for performance reasons) of 48×48 pixels representing a Chinese handwritten character. It is fed to a convolu-

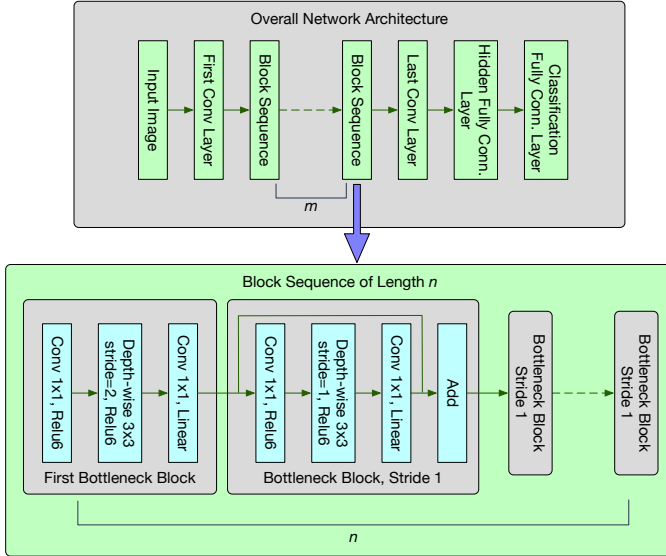


Fig. 1. Adapted MobileNetV2 Architecture.

tion layer, followed by m block sequences, a last convolution layer, and a fully-connected layer before the classification layer. The first and last convolution layer do not perform spatial subsampling. Therefore, spatial subsampling is solely controlled by the number of block sequences. Finally, the classification layer has one node per class, e.g., 3,755 for the Hānzì level-1 subset of GB2312-80, and close to 30,000 when scaled up to the full inventory (cf. Section 3).

At that scale, disk footprint is dominated by the parameters of the fully-connected classification layer. It is very important to control the input dimension of that last layer in order to avoid generating models with a very large number of parameters, which would not only be hard to train but would also have an absurdly large footprint. This can be avoided by using a very conservative number of output units in the last hidden layer. The same reasoning applies as well to the input of the hidden fully-connected layer. Its input dimension can be restricted by stacking a sufficient number of block sequences to decrease the image spatial resolution and by setting a conservative number of channels for the last convolution layer.

Note that, given our product focus, we deliberately do not tune our system for the highest possible accuracy on benchmark datasets. Indeed our priorities are model size, evaluation speed, and user experience. In that context, we opt for a compact system that works in real-time, across a wide variety of styles, and with high robustness towards non-standard stroke order. This leads to an image based recognition approach even though we evaluate it on on-line datasets.

3. SCALING UP TO 30K CHARACTERS

Since the ideal set of “frequently written” characters varies from one user to the next, a large population of users requires an inventory of characters much larger than 3,755. Exactly which ones to select, however, is not entirely straightforward. Simplified Chinese characters defined with GB2312-80 and traditional Chinese characters defined with Big5, Big5E, and CNS 11643-92 cover a wide range (from 3,755 to 48,027 Hānzì characters). More recently came HKSCS-2008 with 4,568 extra characters, and even more with GB18030-2000.

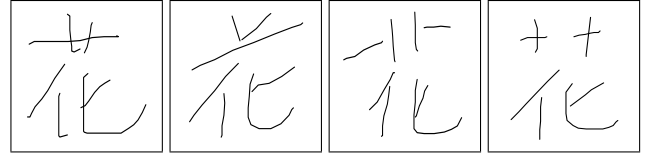


Fig. 2. Printed Radical Variations of U+82B1 (花)

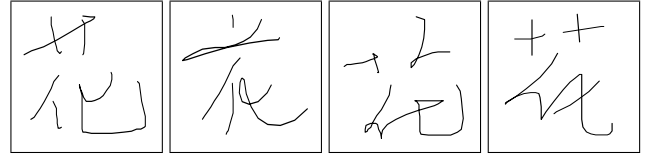


Fig. 3. Cursive Radical Variations of U+82B1 (花)



Fig. 4. Unconstrained Variations of U+82B1 (花)

We opted for the Hānzì part of GB18030-2005, HKSCS-2008, Big5E, a core ASCII set, and a set of visual symbols and emojis, for a total of approximately 30,000 characters, which we felt represented the best compromise for the daily correspondence of most Chinese users.

Upon selection of the character inventory, it is critical to sample the writing styles that users actually use. While there are formal clues as to what styles to expect (cf. [17]), there exist regional variations in writing styles, e.g., (i) the use of the U+2EBF (艹) radical, or (ii) the cursive U+56DB (四) vs. U+306E (㇀). Rendered fonts can also contribute to confusion as some users expect specific characters to be presented in a specific style. As a speedy input tends to drive toward cursive styles, it tends to increase ambiguity, e.g. between U+738B (王) and U+4E94 (五). Finally, increased internationalization sometimes introduces unexpected collisions: for example, a cursively written U+4E8C (二) may conflict with the Latin characters “2” and “Z”.

To cover the whole spectrum of possible input from printed to cursive to unconstrained writing [9], including as many variants as we could, we sought data from a broad spectrum of writers from multiple regions in Greater China. We collected data from paid participants across various age groups, gender, and with a variety of educational backgrounds, thus resulting in tens of millions of character instances for our training data. We were surprised to observe that most users have never seen, let alone written, many of the rarer characters. This unfamiliarity results in hesitations, stroke-order errors, and other distortions which introduce additional complexity, as the data collection needs to capture such distortions in sufficient detail that models can properly encapsulate them.

To illustrate the variety of writing styles we collected, Figs. 2–4 show some examples of the “flower” character for U+82B1 (花). Fig. 2 illustrates the variety in the grass radical on the top, Fig. 3 does the same for cursive, and Fig. 4 for even more unconstrained data.

The fact that, in daily life, users often write quickly and unconstrained can lead to cursive variations that have a very dissimilar appearance. Conversely, sometimes it also leads to confusability between different characters. Just like in English, where a “v” becomes a “u” shape when writing quickly,



Fig. 5. Variations of U+7684 (的)

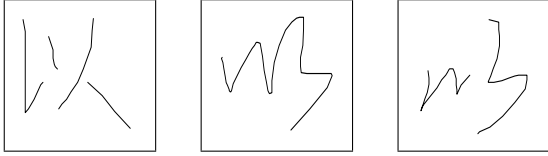


Fig. 6. Variations of U+4EE5 (以)

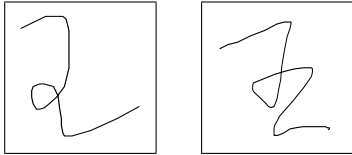


Fig. 7. Similar Shapes of U+738B (王) and U+4E94 (五)

two different Chinese cursive characters could end up looking very similar to each other. Figs. 5–7 show some of the concrete examples we observe in our data. Note that it is especially important to have enough training material to distinguish cursive variations such as in Fig. 7.

4. EXPERIMENTAL RESULTS

4.1. Model optimization

Several MobileNetV2 hyper-parameters require fine-tuning: Table 1 reflects a family of parameters that yields good accuracy. We use the same expansion factor for all the bottleneck blocks. The number of bottleneck block sequences is selected to decrease the spatial resolution of the last feature map and hence decrease the model disk footprint. The number of output channels of the last convolution layer and the number of units of the hidden fully-connected layer are also chosen to limit the model footprint. In addition, we experimented with replacing the fully-connected layer with a global average pooling layer. The sequence length of each bottleneck block is uniformly sampled in the range $[1, \text{max. sequence len.}]$, providing some diversity on the sequence length within a given model. Finally, the numbers of channels of the bottleneck blocks are chosen from the following list $[32, 48, 64, 96, 128, 256]$.

We ensure that the number of channels from one block sequence to the next one never decreases. Starting by the first bottleneck block, the number of output channels is randomly sampled from the first 3 entries of the list. The list is then updated by discarding any values strictly smaller than the sampled value. Next, the number of channels for the next layer is chosen from the updated list. This sampling and list updating process is carried on for all the bottleneck blocks, and the maximum number of channels is restricted to be 256.

We use stochastic gradient descent with Nesterov momentum as optimizer. We found that a learning rate between 0.01 and 0.1 and a batch of size between 250 and 1000 are reasonable choices. Additionally, we supplemented actual observations with suitable elastic deformations as advocated in [13, 15]. Finally, we tried to include attention modules at the output of the bottleneck blocks [18]. However, it did not

Table 1. Model Hyper-Parameters

Hyper-parameters	Values
expansion factor t	$[2, 4, 6, 8]$
nb. block sequence	$[3, 4, 5]$
max. sequence len.	$[2, 4, 6, 8, 10]$
first conv. channels	$[16, 24, 32, 48]$
last conv. channels	$[128, 256]$
fully conn. layer units	$[0, 128, 256]$

provide any immediate accuracy improvement; further investigation is probably warranted but left for future work.

For every training scenario detailed below for various datasets, we launched 50 model configuration trials by randomly sampling hyper-parameters values from Table 1, and reported the accuracy and disk footprint of the best model. On the average, we observed an accuracy delta between the 10 best configurations of 0.6%. In order to showcase the diversity of the model architecture explored, Table 2 and Table 3 show the configurations of the two best models, respectively named type 1 and type 2. It is worth noting that despite being quite different, both models provide a similar level of accuracy. It suggests that there is not a single optimal configuration, but instead a family of configurations that yields high accuracy. Interestingly, the last hidden layer of both these models have 128 units, leading to relatively compact models with a disk footprint of 19MB for the type 1 model and of 17MB for the type 2 model. Similar configurations with 256 units in their last hidden layers exhibit a disk footprint above 30MB.

Table 2. Architecture Type 1

Input	Layer	t	c	n	s
$48 \times 48 \times 1$	conv2D	-	16	1	1
$48 \times 48 \times 16$	bottleneck	8	64	4	2
$24 \times 24 \times 64$	bottleneck	8	64	4	2
$12 \times 12 \times 64$	bottleneck	8	64	4	2
$6 \times 6 \times 64$	bottleneck	8	96	2	2
$3 \times 3 \times 96$	conv2D	-	128	1	1
$3 \times 3 \times 128$	dense	-	128	1	-
128	dense	-	30K	1	-

Table 3. Architecture Type 2

Input	Layer	t	c	n	s
$48 \times 48 \times 1$	conv2D	-	24	1	1
$48 \times 48 \times 24$	bottleneck	4	32	7	2
$24 \times 24 \times 32$	bottleneck	4	64	8	2
$12 \times 12 \times 64$	bottleneck	4	96	4	2
$6 \times 6 \times 96$	conv2D	-	128	1	1
$6 \times 6 \times 128$	global avg. pooling	-	128	1	1
128	dense	-	30K	1	-

4.2. Results on CASIA dataset

Whereas the ultimate goal is to scale up to GB18030-like coverage, it is informative to start by evaluating our MobileNetV2 implementation on a benchmark task such as CASIA [10]. While covering relatively few characters, this task has the merit to have been well-studied in the literature, as reported in, e.g., [11] and [19]. For comparison, we replicated the same setup based on the datasets CASIA-OLHWDB, DB1.0-1.2 [10, 11], split in training and testing datasets, yielding about one million training exemplars.

Table 4 shows the results obtained using the architecture of Fig. 1, where the abbreviation “Hz-1” refers to the Hānzì level-1 inventory (3,755 characters), and “CR(n)” denotes

Table 4. Results on CASIA On-line Database, 3,755 Characters. Standard Training, Associated Model Size = 11MB.

Inventory	Training	CR(1)	CR(4)	CR(10)
H _z -1	CASIA	95.1%	98.9%	99.5%

Table 5. Results on CASIA On-line Database, 3,755 Characters. Augmented Training, Associated Model Size = 13MB.

Inventory	Training	CR(1)	CR(4)	CR(10)
H _z -1	Augmented	96.8%	99.4%	99.7%

top- n character recognition accuracy. Note that we are listing top-4 accuracy in addition to commonly reported top-1 and top-10 accuracies: because our user interface was designed to show 4 character candidates, top-4 accuracy is an important predictor of user experience in our system.

The figures in Table 4 compare with on-line results in [11] and [19] averaging roughly 93% for top-1 and 98% for top-10 accuracy. Thus, our top-1 and top-10 accuracies are in line with the literature. Furthermore, our top-4 accuracy is very satisfactory, and perhaps even more importantly, obtained with a model size (11 MB) on the smaller end of the spectrum among comparable systems in [11] and [19].

The system in Table 4 is trained only on CASIA data, and does not include any other training data. We were also interested in folding in additional training data collected in-house on a variety of devices. As detailed in Section 3, this data covers a larger variety of styles and comprises a lot more training instances per character. Table 5 reports the results observed, on the same test set with a 3,755-character inventory.

The resulting top-1 and top-4 accuracies are 1.7% and 0.5% higher, respectively, when compared to the system in Table 4. Such relatively modest improvement suggests that the various character styles appearing in the test set were already well covered in the CASIA training set. But it also indicates that folding in additional styles has no deleterious effect on the model, which in turn supports looking at learning curves to estimate how the error scales with data size [2]. As is well-known, on a log-log plot the “steepness” of such learning curves empirically conveys how quickly a model can learn from adding more training samples [4].

Finally, Table 6 reports results on the exact same test set for the full system, for which the number of recognizable characters increases from 3,755 to approximately 30,000. Compared to Table 5, accuracy drops—which was to be expected, since the vastly increased coverage creates additional confusability (for example, between 一 and Z as mentioned earlier). Still, the drop remains rather limited, which is encouraging. In fact, a comparison between Tables 5 and 6 shows that multiplying coverage by a factor of 8 entails far less than 8 times more errors, or 8 times more storage. Instead, the increase in both number of errors and model size is confined to manageable values. Thus, building a high-accuracy Chinese character recognition that covers 30,000 characters, instead of only 3,755, is possible and practical.

4.3. Results on in-house dataset

To get an idea of how the full system performs across the entire set of 30,000 characters, we also evaluated the accuracy of the MobileNetV2 architecture of type 1 (Table 2) on a number of different test sets comprising all supported characters written in various styles. As baseline, we opted for the LeNet architecture, as it has been commonly used in previous hand-

Table 6. Results on CASIA On-line Database, 30,000 Characters.

Inventory	CR(1)	CR(4)	CR(10)	Model Size
30K	96.6%	99.3%	99.6%	19MB

Table 7. Average Results on Multiple In-House Test Sets Comprising All Writing Styles, 30,000 Characters.

Model	CR(1)	CR(4)	CR(10)	Model Size
mobileNetV2	97.2%	99.6%	99.8%	19MB
LeNet	92.6%	98.4%	99.2%	15MB

writing recognition experiments on the MNIST task (see, e.g., [1], [13]). The LeNet model is composed of 3 convolution layers, each followed by max pooling, and a fully-connected hidden layer with 128 units, similarly to the MobileNetV2 model. This model has a similar disk footprint as the MobileNetV2 model. Table 7 lists the average results for both models on the in-house test sets. Despite both models having roughly the same number of parameters, the mobileNetV2 model top-1 accuracy is 4.6% higher than the LeNet model. This highlights the progress made by the community in designing CNN architectures in recent years.

Finally, even though the results in Tables 6–7 are not directly comparable since they were obtained on different test sets, they show that top-1 and top-4 accuracies are in the same ballpark across the entire inventory of characters. This was to be expected given the largely balanced training regimen.

5. CONCLUSION

We have discussed the unique challenges involved in recognizing Chinese handwritten characters spanning a large inventory of approximately 30,000 characters, while simultaneously achieving real-time performance and minimizing disk memory footprint. Particular attention has to be paid to data collection conditions, representativeness of writing styles, and training regimen. Our experimental observations show that, with proper care, a high-accuracy handwriting recognition system is practical on mobile devices. Furthermore, accuracy only degrades slowly as the supported inventory increases, as long as training data of sufficient quality is available in sufficient quantity. So, how well would we expect to handle even larger inventories? The total set of CJK characters in Unicode is currently around 75,000 [16], and the ideographic rapporteur group (IRG) keeps on suggesting new additions from a variety of sources. Admittedly, these new characters will be rare (e.g., used in historical names or poetry). Nevertheless, they are of high interest to every person dealing with them.

Learning curves [2, 4] obtained by varying the amount of training data allow for extrapolation of asymptotic values, regarding both what our accuracy would look like with more training data, and how it would change with more characters to recognize. Given the 8-times larger inventory and corresponding (less than) 0.2% drop in accuracy between Table 5 and Table 6, we can extrapolate that with an inventory of 100,000 characters and a corresponding increase in training data, it would be realistic to achieve top-1 accuracies around 96%, and top-10 accuracies around 99% (with the same type of architecture). These figures support recognition feasibility, even on mobile devices. This bodes well for the recognition of even larger sets of Chinese characters in the future.

6. REFERENCES

- [1] D.C. Ciresan, U. Meier, L.M. Gambardella, and J. Schmidhuber, "Convolutional Neural Network Committees For Handwritten Character Classification," in *11th Int. Conf. Document Analysis Recognition (ICDAR 2011)*, Beijing, China, Sept. 2011.
- [2] C. Cortes, L.D. Jackel, S.A. Jolla, V. Vapnik, and J.S. Denker, "Learning Curves: Asymptotic Values and Rate of Convergence," in *Advances in Neural Information Processing Systems (NIPS 1993)*, Denver, pp. 327–334, Dec. 1993.
- [3] K. He, X. Zhang, S. Ren and J. Sun, "Deep Residual Learning for Image Recognition," in *Proc. IEEE Conf. Computer Vision Pattern Recognition (CVPR 2016)*, Las Vegas, NV, pp. 770–778, 2016.
- [4] J. Hestness, S. Narang, N. Ardalani, G. Diamos, H. Jun, H. Kianinejad, M.M.A. Patwary, Y. Yang, and Y. Zhou, "Deep Learning Scaling is Predictable, Empirically," *arXiv:1712.00409v1*, Dec. 2017.
- [5] G.E. Hinton and K.J. Lang, "Shape Recognition and Illusory Conjunctions," in *Proc. 9th Int. Joint Conf. Artificial Intelligence*, Los Angeles, CA, pp 252–259, 1985.
- [6] A.G. Howard, M. Zhu, B. Chen, D. Kalenichenko, W. Wang, T. Weyand, M. Andreetto, and H. Adam, "Mobilenets: Efficient Convolutional Neural Networks for Mobile Vision Applications," *arXiv:1704.04861*, 2017.
- [7] S. Ioffe, and C. Szegedy, "Batch Normalization: Accelerating Deep Network Training by Reducing Internal Covariate Shift," *arXiv:1502.03167*, 2015.
- [8] Y. LeCun, L. Bottou, Y. Bengio, and P. Haffner, "Gradient-based Learning Applied to Document Recognition," *Proc. IEEE*, Vol. 86, No. 11, pp. 2278–2324, Nov. 1998.
- [9] C.-L. Liu, S. Jaeger, and M. Nakagawa, "Online Recognition of Chinese Characters: The State-of-the-Art," *IEEE Trans. Pattern Analysis Machine Intelligence*, Vol. 26, No. 2, pp. 198–213, Feb. 2004.
- [10] C.-L. Liu, F. Yin, D.-H. Wang, and Q.-F. Wang, "CA-SIA Online and Offline Chinese Handwriting Databases," in *Proc. 11th Int. Conf. Document Analysis Recognition (ICDAR 2011)*, Beijing, China, Sept. 2011.
- [11] C.-L. Liu, F. Yin, Q.-F. Wang, and D.-H. Wang, "ICDAR 2011 Chinese Handwriting Recognition Competition" in *11th Int. Conf. Document Analysis Recognition (ICDAR 2011)*, Beijing, China, Sept. 2011.
- [12] Y. Li, L. Jin , X. Zhu, T. Long, "SCUT-COUCH2008: A Comprehensive Online Unconstrained Chinese Handwriting Dataset (ICFHR 2008)," Montreal, pp. 165–170, Aug. 2008.
- [13] U. Meier, D.C. Ciresan, L.M. Gambardella, and J. Schmidhuber, "Better Digit Recognition with a Committee of Simple Neural Nets," in *11th Int. Conf. Document Analysis Recognition (ICDAR 2011)*, Beijing, China, Sept. 2011.
- [14] M. Sandler, A. Howard, M. Zhu, A. Zhmoginov, and L.-C. Chen, "MobileNetV2: Inverted Residuals and Linear Bottle-necks," in *Proc. IEEE Conf. Computer Vision Pattern Recognition (CVPR 2018)*, pp. 4510–4520, 2018.
- [15] P.Y. Simard, D. Steinkraus, and J.C. Platt, "Best Practices for Convolutional Neural Networks Applied to Visual Document Analysis," in *7th Int. Conf. Document Analysis Recognition (ICDAR 2003)*, Edinburgh, Scotland, Aug. 2003.
- [16] Unicode, *Chinese and Japanese*, http://www.unicode.org/faq/han_cjk.html, 2015.
- [17] F.F. Wang, *Chinese Cursive Script: An Introduction to Handwriting in Chinese*, Far Eastern Publications Series, New Haven, CT: Yale University Press, 1958.
- [18] F. Wang, M. Jiang, C. Qian, S. Yang, C. Li, H. Zhang, X. Wang, and X. Tang, "Residual Attention Network for Image Classification," in *Proc. IEEE Conf. Computer Vision Pattern Recognition (CVPR 2017)*, pp. 3156–3164, 2017.
- [19] F. Yin, Q.-F. Wang, X.-Y. Xiang, and C.-L. Liu, "ICDAR 2013 Chinese Handwriting Recognition Competition" in *11th Int. Conf. Document Analysis Recognition (ICDAR 2013)*, Washington DC, USA, Sept. 2013.